# Enhancing Cell Nucleation of Thermoplastic Polyolefin Foam Blown with Nitrogen

**S. G. Kim,[1] J. W. S. Lee,[2] C. B. Park,[2] M. Sain[1]**

[1]*Department of Chemical Engineering & Applied Chemistry, University of Toronto, Toronto, Ontario M5S 3E5, Canada*
[2]*Department of Mechanical & Industrial Engineering, University of Toronto, Toronto, Ontario M5S 3G8, Canada*

Received 20 March 2009; accepted 4 December 2009
DOI 10.1002/app.32294
Published online 7 June 2010 in Wiley InterScience (www.interscience.wiley.com).

**ABSTRACT:** More than ever before, thermoplastic polyolefin (TPO) is actively used for interior and exterior applications in the automotive industry. Foamed TPO parts use far less material than their solid counterparts and, thereby, reduce material cost, weight, and fuel usage. However, foamed TPO is not yet in mainstream use because the appropriate foaming technology is not yet well developed. The literature reports the use of carbon dioxide ($CO_2$) as a blowing agent for TPO;[1–3] there is, however, little research on the use of nitrogen ($N_2$) as a blowing agent, despite nitrogen's numerous advantages. In this study, various talc contents were added to a TPO matrix consisting of polypropylene blended with a metallocene-based polyolefin elastomer. The effect of talc on the TPO foams blown with $N_2$ was studied with a batch foaming simulation system. The simulated results were compared actual foam extrusion results. The influence of the $N_2$ content and processing conditions on the cell nucleation behavior is discussed. © 2010 Wiley Periodicals, Inc. J Appl Polym Sci 118: 1691–1703, 2010

**Key words:** foam extrusion; nucleation; simulations

## INTRODUCTION

Thermoplastic polyolefins (TPOs) are composite blends of semicrystalline polypropylene (PP) and ethylene–propylene copolymer or ethylene–propylene–diene monomer and are widely used in the automotive industry for the production of plastic car parts, such as bumper fascia.[4] PP, which is the major component of such blends, is an inexpensive, easily processable polymer, although its poor mechanical properties necessitate the addition of a rubber-dispersed phase. The added rubber acts as an impact modifier by imparting improved ductility, crack resistance, and impact strength to the resulting TPO.[4–7] The cost effectiveness, light weight, processability, and resilience of TPOs have made them increasingly viable alternatives to steel for bumpers and other car parts.

In recent years, metallocene-based polyolefin elastomers (POEs), such as ethylene–octane copolymer (EOC), have replaced the customary ethylene–propylene copolymer and ethylene–propylene–diene monomer because of their comparable molecular weights and improved compatibility with PP; both these qualities lead to submicrometer dispersions of POEs in high-flow-rate PP.[8] The availability of TPO products containing POEs presents a low-cost alternative for achieving balanced material performance.[9]

However, foamed TPO has not been incorporated into mainstream use because the technology for foaming TPO with extrusion or injection molding is not yet well developed. Also, the absence of detailed knowledge about the material properties of TPOs, because of the complexity of their formulations, prevents successful foaming of TPO. Interest is increasing in the development of foamed TPO products to reduce material costs and fuel usage in automobiles. Polymer foaming technology can effectively reduce material consumption with a minimum deterioration of physical and mechanical properties.

Much research has focused on polymeric foams blown with carbon dioxide ($CO_2$) because $CO_2$ offers advantages such as inertness, nontoxicity, and nonflammability.[1–3] On the other hand, very limited research has been conducted on the effectiveness of nitrogen ($N_2$) as a blowing agent in the foaming process as compared that of to $CO_2$. There are three main advantages to using $N_2$ over $CO_2$. First, the cell density per weight percentage of blowing agent is higher for $N_2$ than for $CO_2$.[10–12] Second, the specific volume of $N_2$ is higher than $CO_2$, which, in turn, results in a higher expansion ratio per weight

*Correspondence to:* C. B. Park (park@mie.utoronto.ca).
Contract grant sponsors: AUTO21, Natural Science and Engineering Research Council of Canada, Consortium for Cellular and Micro-Cellular Plastics.
Part of this article was presented at the Annual Technical Conference 2007, Cincinnati, Ohio, May 2007.

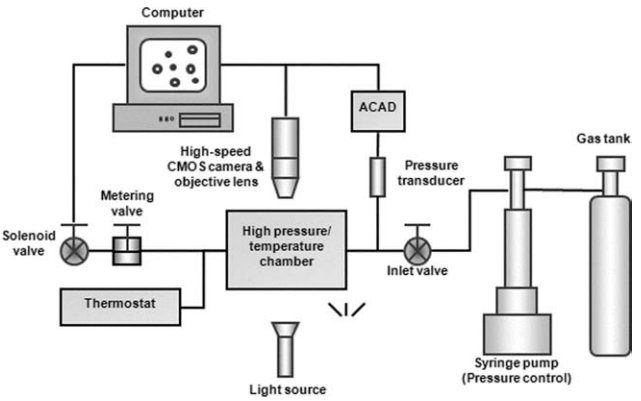


**Figure 1** Schematic of the batch foaming simulation system.

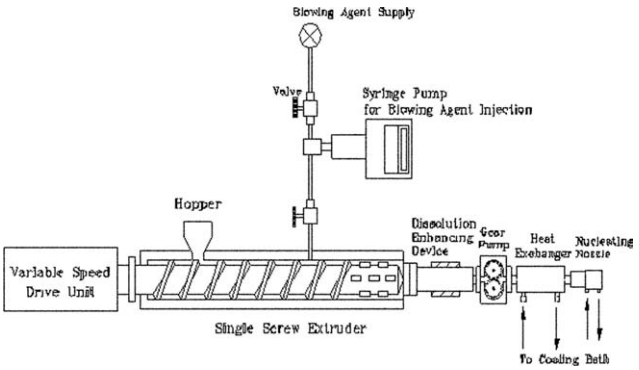


**Figure 2** Schematic of the single-extrusion system.

percentage of blowing agent. Finally, foams blown with $N_2$ shrink less because $N_2$ is the main component of atmospheric gas, and so the diffusion rate of atmospheric gas in the foams is almost same as that of the blowing agent ($N_2$) out of the foams. These facts motivated our investigation into the behavior of $N_2$ as a blowing agent in the foaming process.

The nucleating agent used in foam processing plays an important role in determining the foam's cellular structure. Usually, nucleating agents are fine powders and serve as solid surfaces for heterogeneous cell nucleation; they remain solid or thermally stable during the foaming process. The nucleating agents commonly used in plastic foam processing include calcium stearate, magnesium silicate, zinc stearate, talc, sodium benzoate, stearic acid, silicate products, calcium carbonate, rubber particles, and the mixture of citric acid and sodium bicarbonate.[13] The cellular structure is usually unacceptable without the addition of a nucleating agent, unless a great deal of thermodynamic instability via a rapid solubility drop is induced to promote a large number of nuclei.[14,15] If a nucleating agent is not added, the cell density becomes too low, and the bubbles become too large. Moreover, even a small amount of nucleating agent can significantly lower the processing pressure and pressure-drop rates required for the production of foam with a high cell density.[14,15] Obtaining a high cell density at a lower pressure and with a smaller pressure-drop rate by the simple addition of a small amount of nucleating agent/additive is advantageous. In this study, talc was used as a nucleating agent to control the cell density in the TPO matrix on the basis of heterogeneous nucleation.

The final cell structure observed from scanning electron microscopy (SEM) images may not be the same as the initial nuclei density because of the active cell-coalescence and cell-ripening phenomena taking place in the actual foaming processes, such as injection, extrusion, and compression molding. Therefore, it is difficult to understand what is happening during the beginning stages of the foaming process through only on the final SEM micrographs. Moreover, because of the numerous parameters that play roles in the actual foaming process, it has been difficult to identify the fundamental mechanisms of cell nucleation and cell expansion with processing equipment.[16,17] To better understand the nature of various foaming mechanisms, a visual observation system is, therefore, needed to detect how the bubbles nucleate and grow at the beginning stages of foaming. Using a visual observation high-pressure cell, Taki and coworkers[18,19] recently studied the dynamic behavior of bubble nucleation in the batch physical foaming of PP and PP–clay nanocomposites. In this study, the foamability of TPO–talc composites was evaluated with a newly designed batch foaming simulation with visualization capabilities.[20] The dynamic behavior of the early stage of foaming was investigated. Employing image-processing techniques, we analyzed the bubble nucleation for different composites from the foaming images. The cell nucleation of the TPO materials was studied with talc as a nucleating agent.

For high-density foams, the achievable void fraction is limited by the magnitude of stiffness required; for example, too high a void fraction will result in a lower stiffness, which may compromise the viability of the product. Therefore, the achievable void fraction, which translates into the savings in material costs that can be realistically achieved without jeopardizing the quality of the final product, is determined by the stiffness variable. So far, chemical blowing agents have been mostly used in high-density foam extrusion.

**TABLE I**
**Summary of the Filamentary Dies**

| | Die geometry (length/diameter; in.) | Pressure-drop rate (MPa/s) |
|---|---|---|
| Die 1 | 2.200/0.055 | $\sim$ 30 (low $dP/dt$) |
| Die 2 | 0.400/0.025 | $\sim$ 800 (high $dP/dt$) |

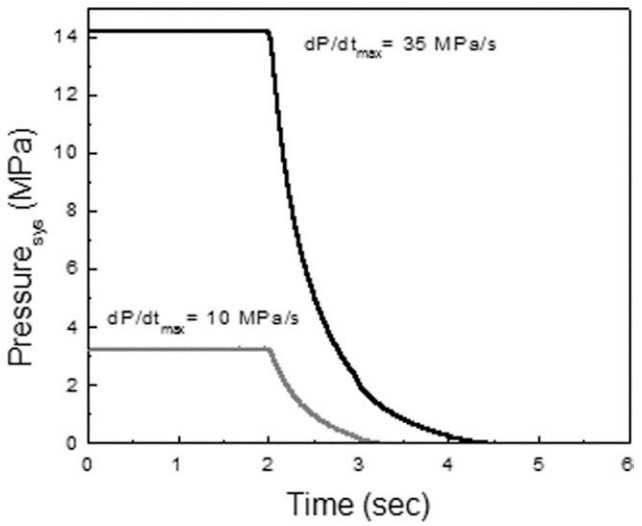


**Figure 3** Pressure profiles in the batch foaming simulation chamber.

However, chemical blowing agents are usually more expensive than physical blowing agents in terms of their operational costs, although the capital costs are higher for physical blowing agents.[21]

In this study, high-density foaming experiments were carried out with TPO as the polymeric material and $N_2$ as the physical blowing agent. In these experiments, we aimed to clarify how the void fraction and cell density changed in response to variations in the die temperature, talc content, blowing agent content, and pressure-drop rate when a physical blowing agent was used. Moreover, we demonstrated that foaming is a crucial means of reducing resin use in plastics manufacturing.[21]

We were specifically interested in the effect of talc on the cell density of the TPO foams when $N_2$ was used as a blowing agent. In this article, we report the foam extrusion results performed with TPO to verify the validity of the batch foaming simulation result. The extrusion experimental results are compared with the simulated results.

## EXPERIMENTAL

### Materials

The PP (PP 7805) used in this study was supplied by Exxon (Bayway, NJ); it had a melt flow index of 80 g/10 min and a density of 0.91 g/cm$^3$. Engage 8130, a metallocene-catalyzed copolymer comprised of ethylene and 1-octene containing 25 wt % of a comonomer, was provided by Dow Chemical; it had a melt flow index of 13 g/10 min and a density of 0.863 g/cm$^3$. Luzenac provided talc; the grade was JetFil700C with a density of 2.8 g/cm$^3$ and an average particle size of 1.5 μm. $N_2$ (99.5% purity) was supplied by Linde Gas Canada (formerly BOC Canada) and was used as a physical blowing agent.

### Preparation of the TPO/talc compounds

First, TPO blends of 70 wt % PP and 30 wt % metallocene-catalyzed EOC were prepared with a corotating twin-screw extruder with a screw diameter of 30 mm (Werner & Pfleiderer ZSK-30 (Stuttgart, Germany), length/diameter ratio = 38 : 1). A master batch of 20 wt % talc was prepared with the same extruder. TPO was then dry-blended with the talc master batch in three different ratios, 95 : 5, 75 : 25,

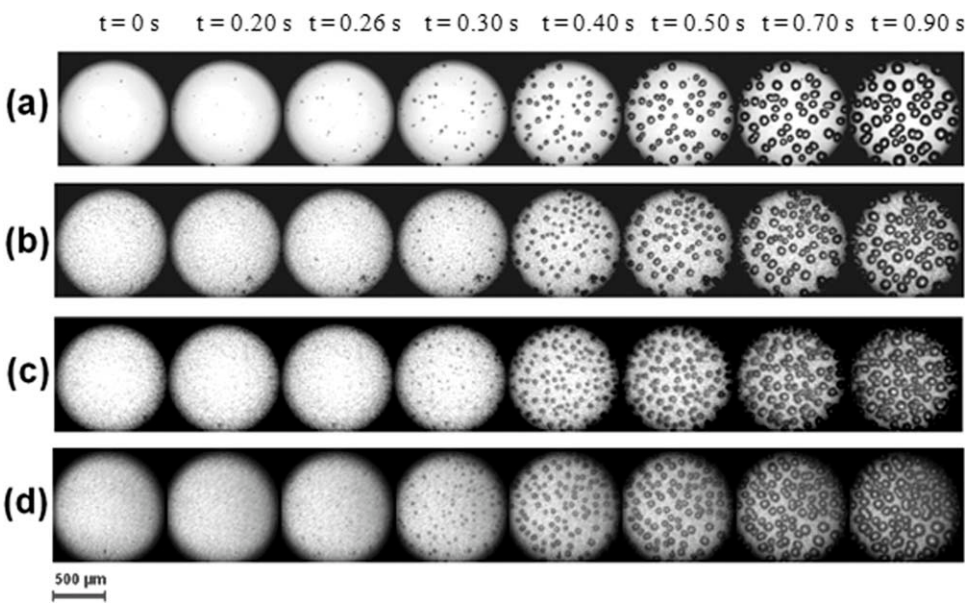


**Figure 4** Serial images of the TPO foaming with $N_2$ with increasing talc content at a high concentration (~ 1.5 wt %) of $N_2$: (a) 0, (b) 1, (c) 5, and (d) 10 wt % talc ($P_{sat}$ = 13.8 MPa, temperature = 180°C, $dP/dt$ = 35 MPa/s).

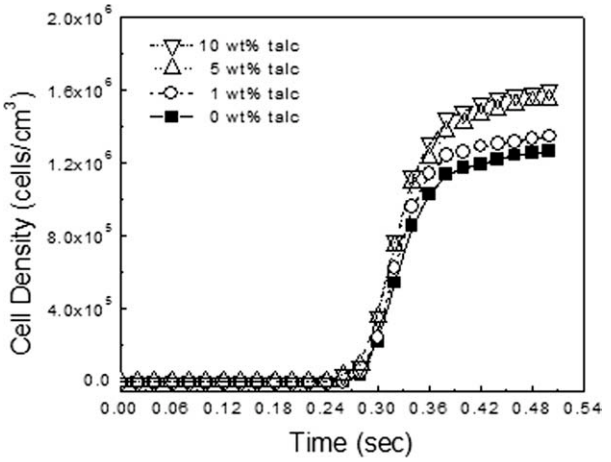


(a) Change in cell density against time

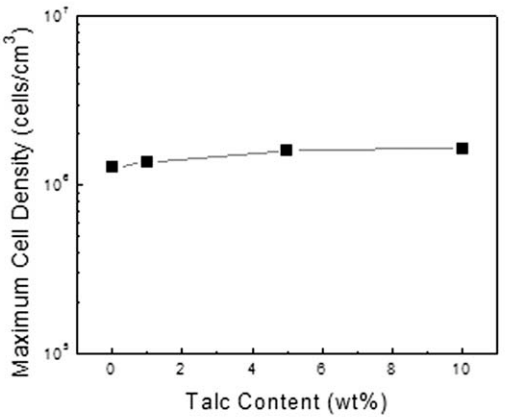


(b) Maximum cell density vs. talc content

**Figure 5** Effect of the talc content on the cell density at a high concentration (~ 1.5 wt %) of $N_2$ ($P_{sat}$ = 13.8 MPa, temperature = 180°C, $dP/dt$ = 35 MPa/s).

and 50 : 50, to produce TPO–talc compounds with talc contents of 1, 5, and 10 wt %, respectively.

### Batch foaming simulation

#### Setup of the visualization system

For the purpose of this experiment, a batch-foaming simulation system containing a high-pressure chamber and a solenoid valve was used.[20] The simulation system consisted of a high-pressure, high-temperature chamber; a pressure-drop rate control system; a data-acquisition system for acquiring pressure measurements (ADAC board); a gas supplier (gas tank, syringe pump, and valves); an objective lens; a light source; and a high-speed, charge-coupled device camera. A schematic of the setup is shown in Figure 1.

#### Experimental procedure

A LabVIEW program (National Instruments, Austin, TX) was used to control the foaming process in the visualization system. The procedure for measuring the pressure decay and for recording the foaming images was as follows:

1. Gas was pumped at a given pressure into the high-pressure–temperature chamber with a syringe pump.
2. The gas temperature inside the chamber was controlled with a thermostat.
3. The solenoid valve was opened, and the pressure decay was recorded with the LabVIEW program.
4. We analyzed the pressure-drop rate on basis of the recorded pressure decay data and

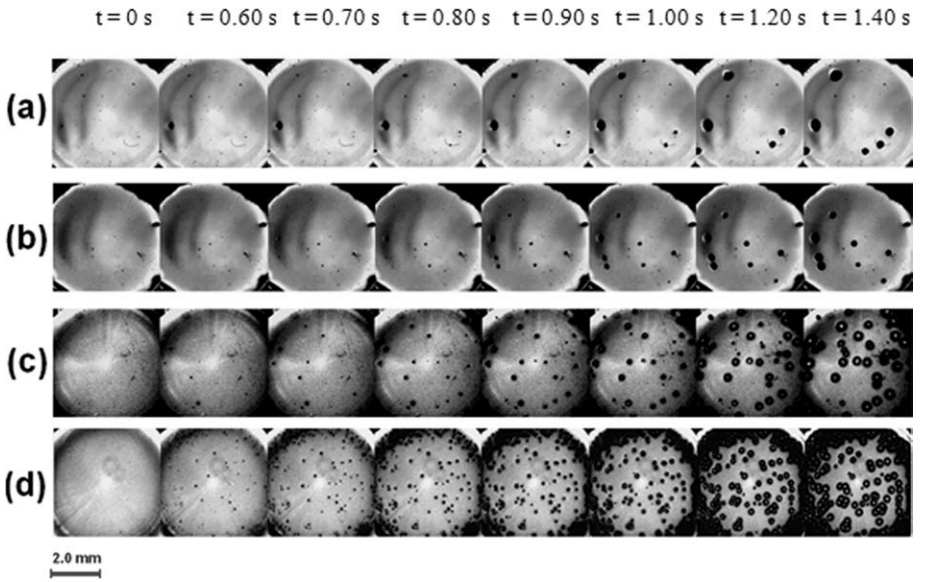


**Figure 6** Serial images of TPO foaming with $N_2$ with increasing talc content at a low concentration (~ 0.4 wt %) of $N_2$: (a) 0, (b) 1, (c) 5, and (d) 10 wt % talc ($P_{sat}$ = 3.45 MPa, temperature = 180°C, $dP/dt$ = 10 MPa/s).

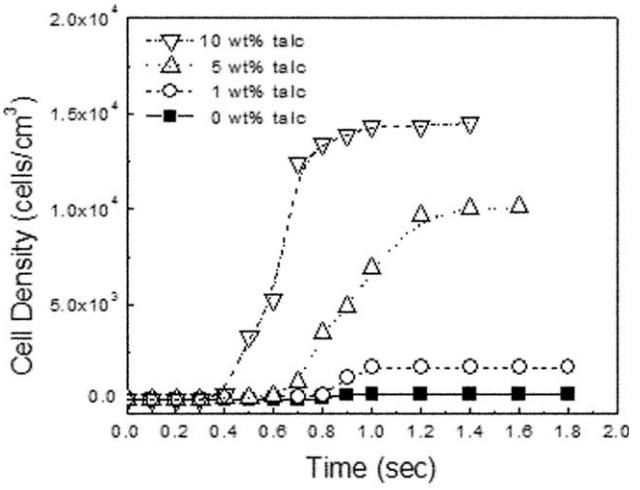


(a) Change in cell density against time

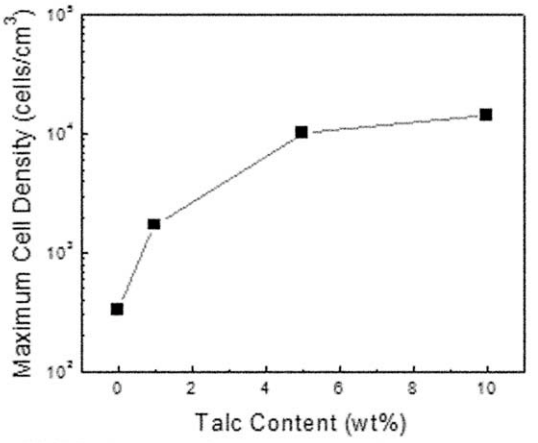


(b) Maximum cell density vs. talc content

**Figure 7** Effect of the talc content on the cell density at a low concentration ($\sim$ 0.4 wt %) of $N_2$ ($P_{sat}$ = 3.45 MPa, temperature = 180°C, $dP/dt$ = 10 MPa/s).

evaluated the bubble nucleation and growth using Image-Pro Plus software (Media Cybernetics, Bethesda, MD).

Analysis of the images

The images captured with the high-speed, charge-coupled device camera were analyzed with Image-Pro Plus software. We calculated the cell density by counting the number of cells in an image at a given moment in time:

$$N = \left(\frac{N_0}{A}\right)^{\frac{3}{2}}\Phi = \frac{\left(\frac{N_0}{A}\right)^{\frac{3}{2}}}{1 - \left[\left(\frac{N_0}{A}\right)^{\frac{3}{2}}\frac{4\pi}{3}R_{avg}^3\right]} \quad (1)$$

where $N$ is the calculated cell density, $N_0$ is the number of cells in an area ($A$) of an image, $\Phi$ is the expansion ratio, and $R_{avg}$ is the volume-average radius of all counted cells at a given moment.[19]

**Foam extrusion**

Experimental setup

Figure 2 shows a schematic of the extrusion foaming system used in the experiment. A single screw extruder (Brabender, 05-25-000, South Hackensack, NJ) with a mixing screw (Brabender, 05-00-144) with a 30 : 1 length/diameter ratio and a 0.75-in. diameter was used. A positive displacement pump was used to inject the physical blowing agent. The other systems included a gear pump (Zenith, PEP-II 1.2 cc/rev), where the volumetric displacement was controlled by a motor, and a heat exchanger for cooling the polymer melt that contained homogenizing static mixers (Labcore model H-04669-12). A filamentary die was also used in this single extruder.

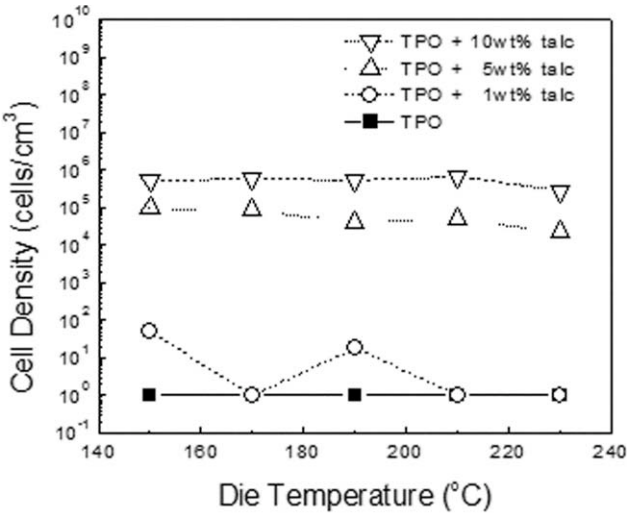


(a)

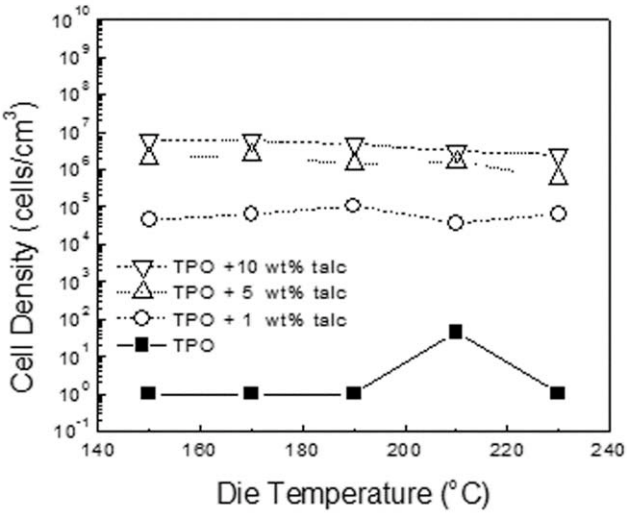


(b)

**Figure 8** Effect of the die temperature on the cell density of the TPO foam with various talc contents (0.1 wt % $N_2$): (a) die 1: low $dP/dt$ and (b) die 2: high $dP/dt$.

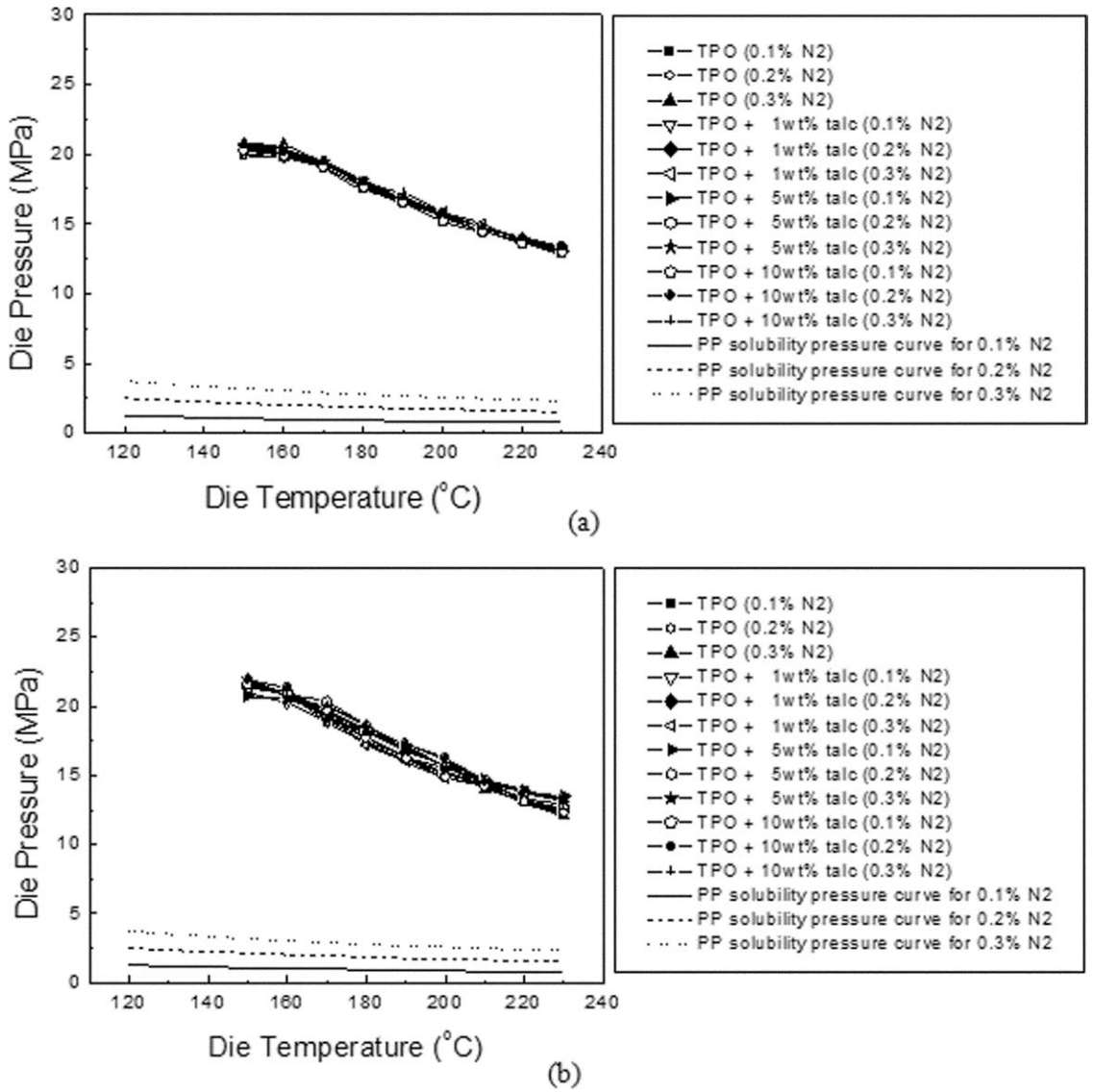


**Figure 9** Die pressure plotted against the die temperature. (a) die 1: low $dP/dt$ and (b) die 2: high $dP/dt$.

## Design of the dies

To observe the effect of the pressure-drop rates on the TPO foams, two different filamentary dies were designed to have the same pressure drops but different pressure-drop rates (see Table I). The detailed design procedure for manufacturing these dies is described in refs. 2 and 14. The procedure for determining the geometry of the two dies had two steps. First, the volumetric flow rate was first set to $1.5 \times 10^{-7}$ $m^3/s$, which remained the typical flow rate value for the extrusion system throughout this study. Subsequently, two different pressure-drop rates, 30 and 800 MPa/s, were selected.

## Experimental procedure

TPO compounds were processed with the foaming extruder with an injection of $N_2$. The experiments were carried out with the two dies at three different levels of $N_2$ (0.1, 0.2, and 0.3 wt %), and the die temperature was carefully decreased from 230 to 130°C at decrements of 10°C. As the temperature decreased, the steady-state pressure changes were recorded for each set of processing conditions. The foam samples were randomly selected at each set of processing conditions and were subsequently characterized.

## Characterization of the foams

The void fraction and cell density were used to characterize the foam samples. The foam density was determined by the water displacement method (ASTM D 792-00). The expansion ratio was calculated as the ratio of the bulk density of TPO compounds and the measured density of the foam sample. The void fraction or weight reduction was determined by

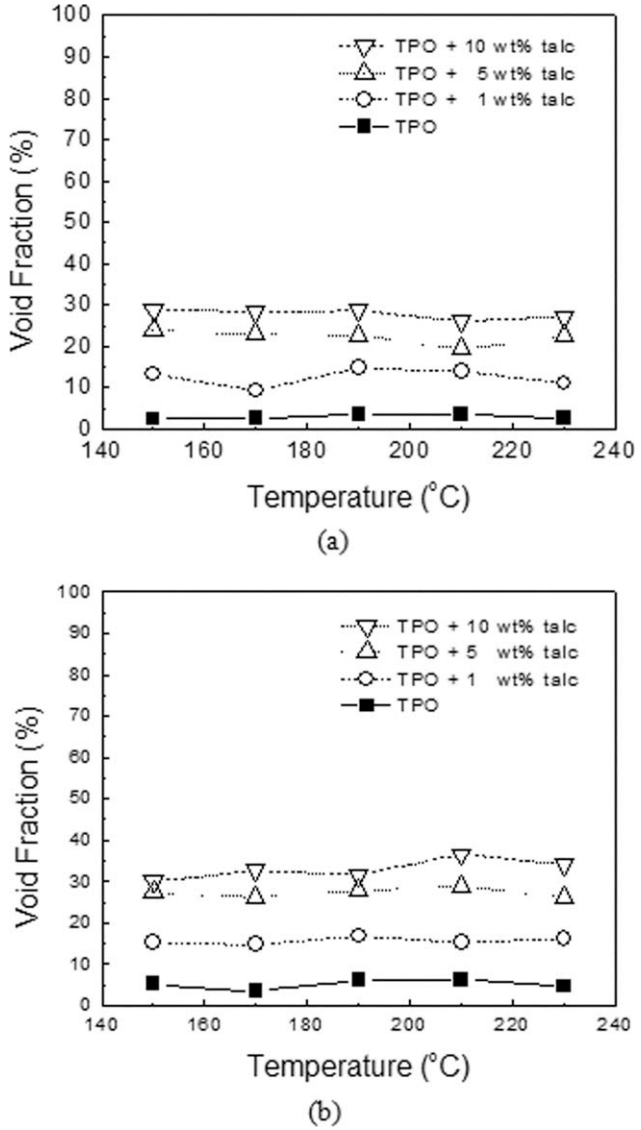


**Figure 10** Effect of the die temperature on the void fraction of the TPO foam with various talc contents (0.1 wt % $N_2$): (a) die 1: low $dP/dt$ and (b) die 2: high $dP/dt$.

$$\text{Void fraction} = \left(1 - \frac{1}{\Phi}\right) \times 100\% \tag{2}$$

The cell density was calculated on the basis of the micrograph obtained by SEM. The samples were first dipped in liquid nitrogen and then fractured to expose their cellular morphology. The fracture surfaces were then gold-coated with a sputter coater to enhance their conductivity, and the microstructures were examined with a JEOL JSM-6060 instrument (Tokyo, Japan). The cell densities were then determined by the following equation:[22]

$$N = \left(\frac{N_0}{A}\right)^{\frac{3}{2}} \Phi = \left(\frac{nM^2}{A}\right)^{\frac{3}{2}} \Phi \tag{3}$$

where $n$ is the number of bubbles in the micrograph, $A$ is the area of the micrograph, and $M$ is the magnification factor of the micrograph.

## RESULTS AND DISCUSSION

### Batch foaming simulation

Figure 3 shows the pressure-drop profiles during the batch foaming experiment under the two different saturation pressures ($P_{sat}$) and pressure-drop rates. The foaming temperature throughout the experiment was 180°C. The pressure in the chamber was released from the saturation pressures, 13.8 MPa (~ 2000 psi) and 3.45 MPa (~ 500 psi), respectively. Although we

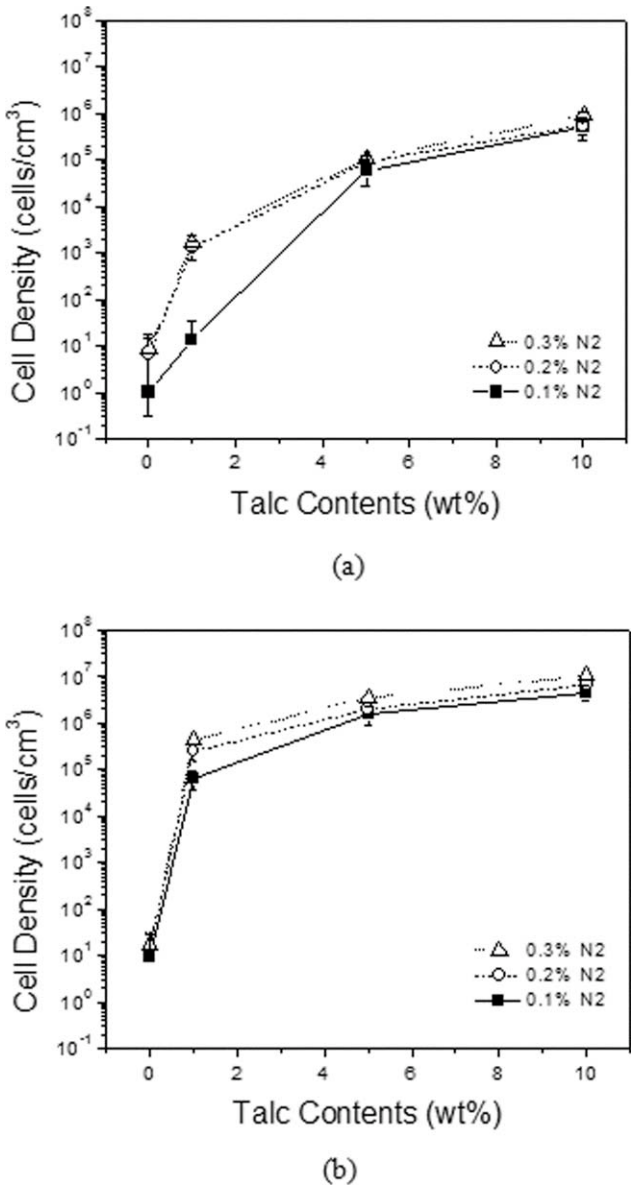


**Figure 11** Effect of the talc content on the cell density of the TPO foam blown with various $N_2$ contents: (a) die 1: low $dP/dt$ and (b) die 2: high $dP/dt$.

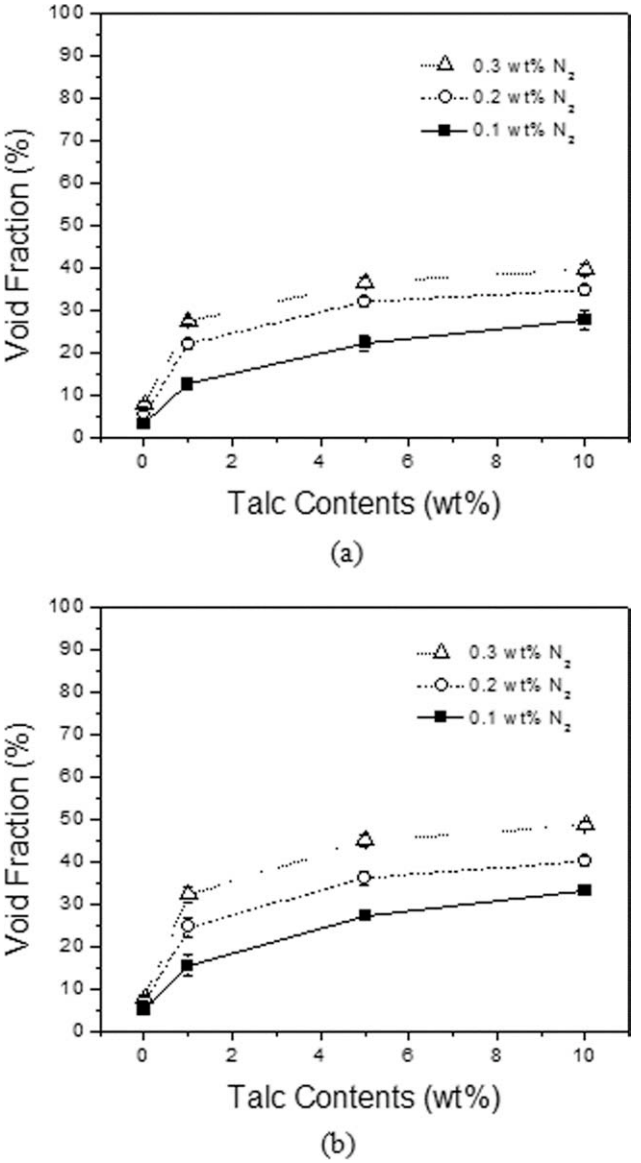


**Figure 12** Effect of the talc content on the void fraction of the TPO foam blown with various $N_2$ contents: (a) die 1: low $dP/dt$ and (b) die 2: high $dP/dt$.

wanted a constant pressure-drop rate, this was difficult to achieve in practice.[20] In this study, the maximum value of the pressure-drop rate is denoted as the pressure-drop rate of each process. The maximum pressure-drop rates calculated for 13.8 and 3.45 MPa were 35 and 10 MPa/s, respectively.

To evaluate the effect of talc on cell nucleation, the pressure profiles were carefully controlled so that every experiment experienced the same pressure conditions. From the measurements of Li et al.[23] the solubility of $N_2$ at 13.8 MPa was about 1.7 wt % for linear PP and about 1.5 wt % for EOC, and the solubility of $N_2$ at 3.45 MPa was about 0.4 wt % for linear PP and about 0.3 wt % for EOC. The solubility of the PP/EOC blend could be estimated with a weighted average.

Figure 4 demonstrates the foaming images generated for the TPO–talc blends with the high-magnification lenses (125×). Figure 5 shows the cell density change against time [Fig. 5(a)] and the maximum cell density with increasing talc content [Fig. 5(b)]. The saturation pressure of $N_2$ was 13.8 MPa, and the pressure-drop rate was 35 MPa/s. The figures show the dynamic behavior of bubble nucleation and growth in the very early stages of physical foaming. The black dots are bubbles, and the white is the TPO matrix. The bubbles in the images appear black because they reflected the light entering from the window on the opposite side of the high-pressure cell. All of the pictures clearly indicate that bubble nucleation and growth occurred simultaneously. The cell density curve shows a sigmoid function shape for all experiments: after an induction time, the nucleation started,

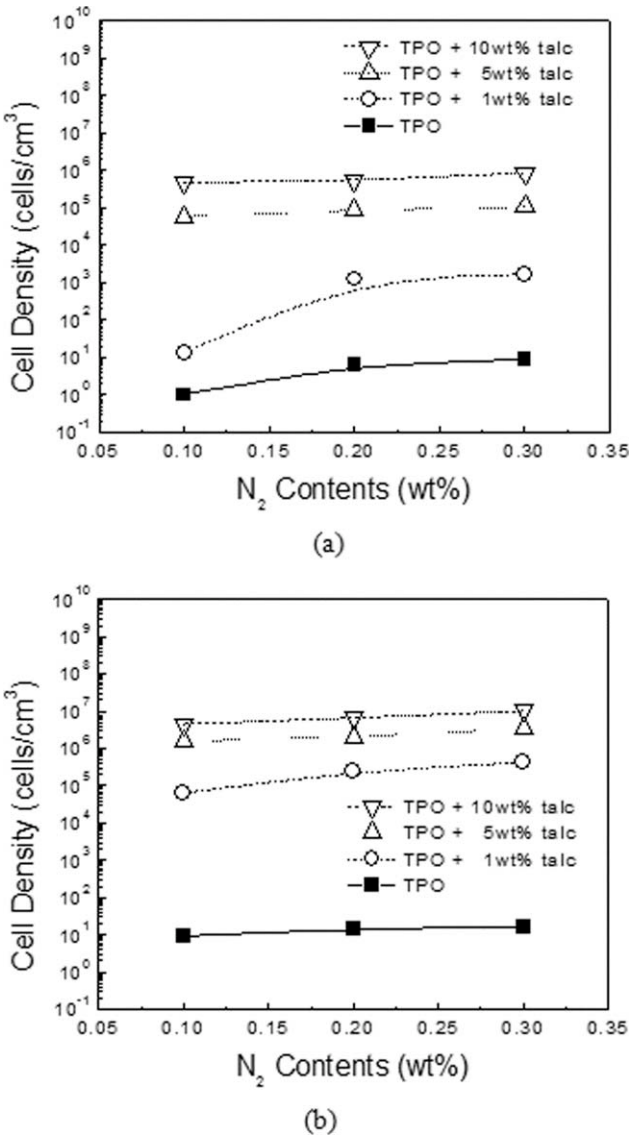


**Figure 13** Effect of the $N_2$ content on the cell density of the TPO foam blown with various $N_2$ contents: (a) die 1: low $dP/dt$ and (b) die 2: high $dP/dt$.

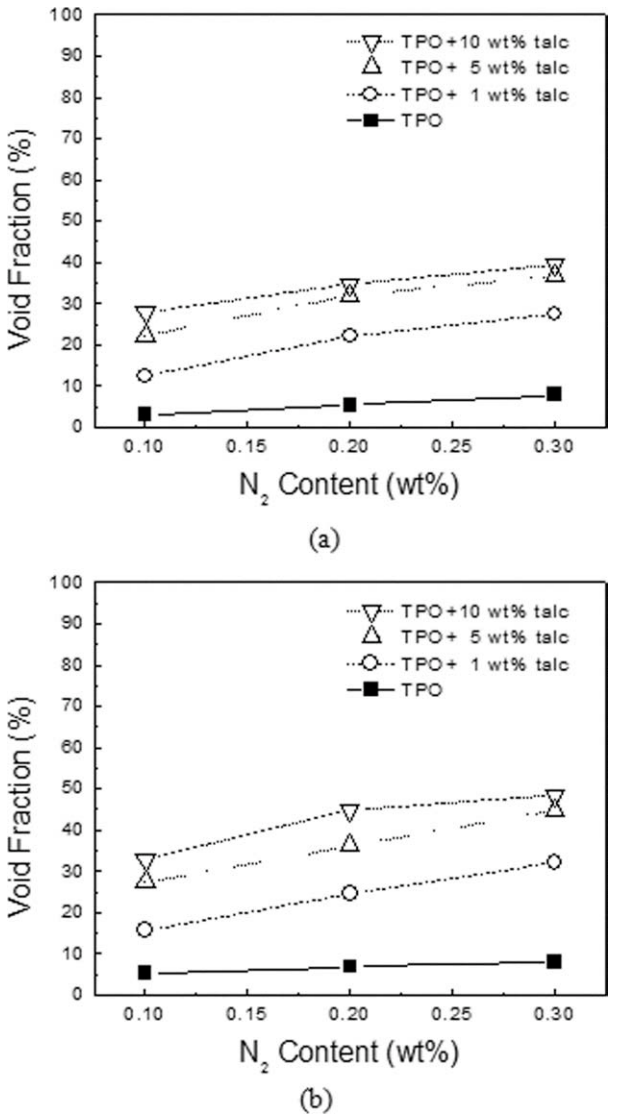


**Figure 14** Effect of the $N_2$ content on the void fraction of the TPO foam blown with various $N_2$ contents: (a) die 1: low $dP/dt$ and (b) die 2: high $dP/dt$.

and the number of bubbles increased. At a certain moment, the nucleation increased dramatically and then ceased. The maximum cell density was where the cell density curve reached a steady state.

Because of bubble coalescence, the maximum cell density may not have been equal to the cell density of the final foam product. To evaluate the nucleation rate in a quantitative way, the foaming images were analyzed with image-processing techniques. We calculated the cell density by counting the number of bubbles observed in an image and applying eq. (1).

Although the cell density did increase with increasing talc content, the difference in density was not noticeable. That is, for TPO/talc systems, the effect of talc was not dominant for the $N_2$ content ($\sim$ 1.6 wt %) and pressure-drop rates ($\sim$ 35 MPa/s) used in this experiment, even though talc has proven to be an effective cell-nucleating agent for many combinations of plastics and blowing agents.[21,24] The cell density increased slightly when the talc content was increased from 0 to 1%, and a further increase was observed when the talc content was increased from 1 to 10%. However, the effect of the talc was not significant. As a result, the sensitivity of the cell density with respect to the talc content was not high for large amounts of $N_2$ because a homogeneous nucleation scheme by a gas dissolved in the polymer matrix was more dominant than the heterogeneous nucleation scheme by the talc particles.

Figure 6 shows foaming images generated for the TPO–talc blends with the low-magnification lenses. Figure 7 shows the cell density change against time [Fig. 7(a)] and maximum cell density with increasing talc content [Fig. 7(b)]. The saturation pressure of $N_2$ was 500 psi, and the pressure-drop rate was 10 MPa/s. These results indicate that cell nucleation was mainly determined by the talc content. The introduction of a small amount of talc significantly

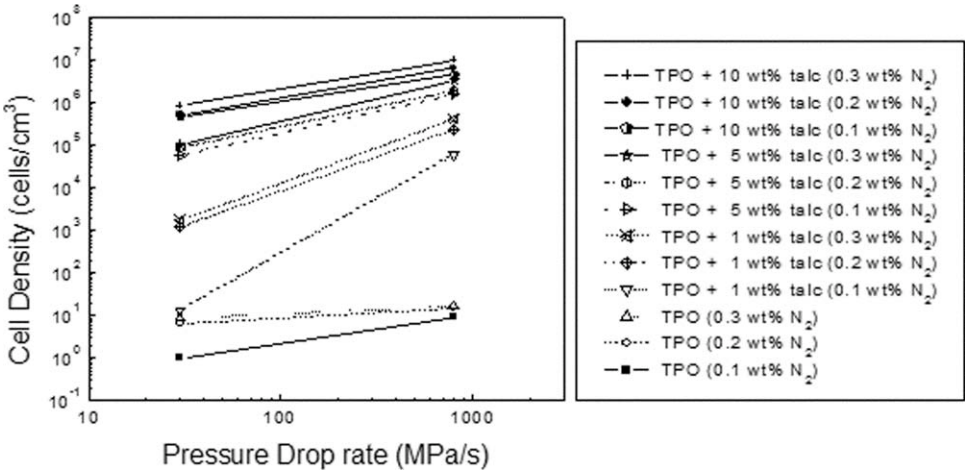


**Figure 15** Effect of the pressure-drop rate on the cell density of the TPO foams.

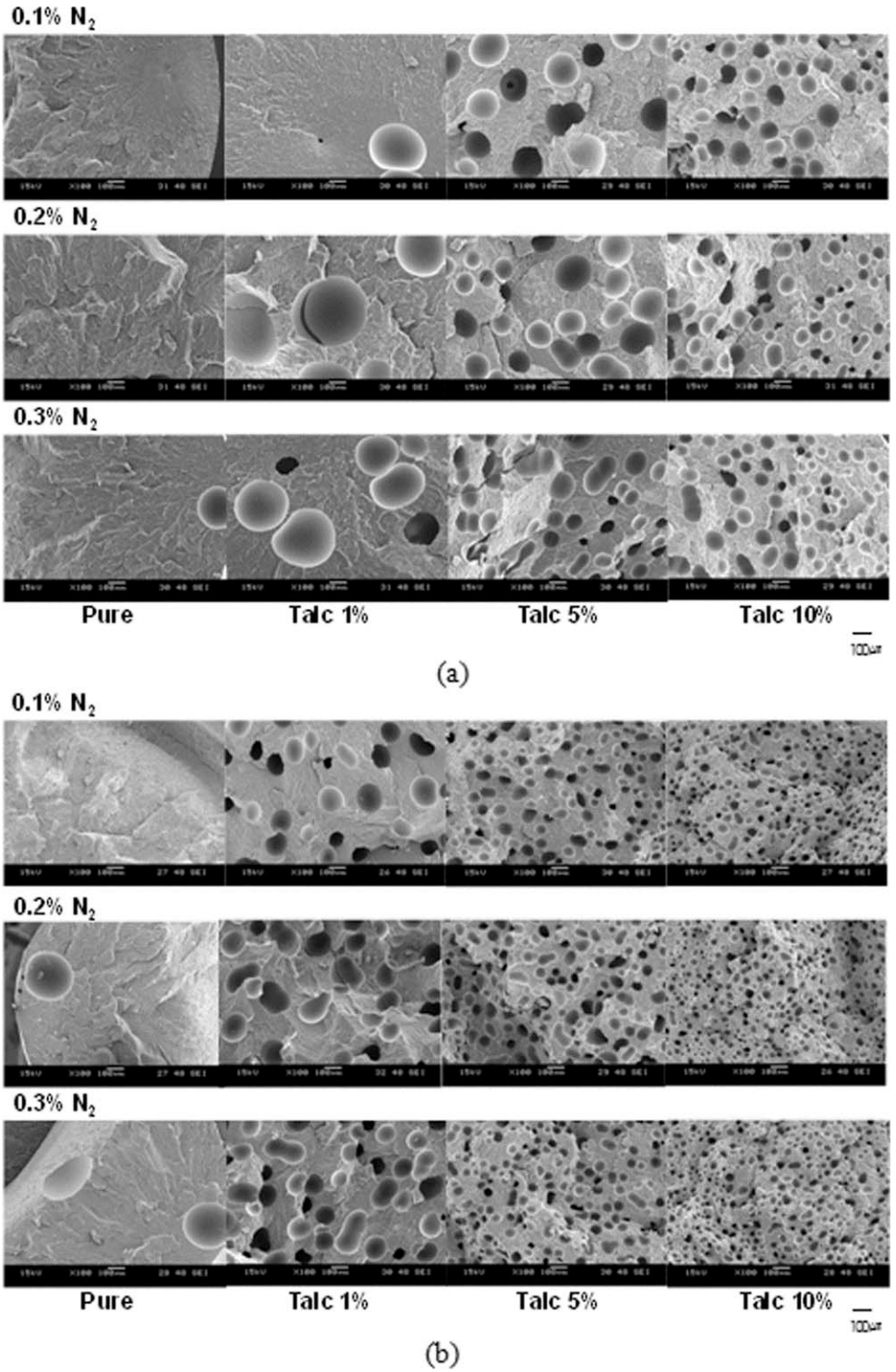


**Figure 16** Cell morphology of the TPO foams blown with $N_2$: (a) die 1: low $dP/dt$ and (b) die 2: high $dP/dt$.

reduced the activation energy barrier and caused a significant increase in bubble nucleation sites. This indicates that talc was a very effective nucleating agent when $N_2$ was used as a blowing agent. Even a small number of talc particles enhanced the cell density by an order of magnitude when the $N_2$ saturation pressure was fixed. Furthermore, when 10 wt % talc particles were added to the TPO matrix, the cell density improved by approximately two orders of magnitude. Comparing these results to those discussed previously, we found that the effect of talc on cell nucleation was significant only at low concentrations of $N_2$ and that the use of talc may not have effectively increased the cell density at a high

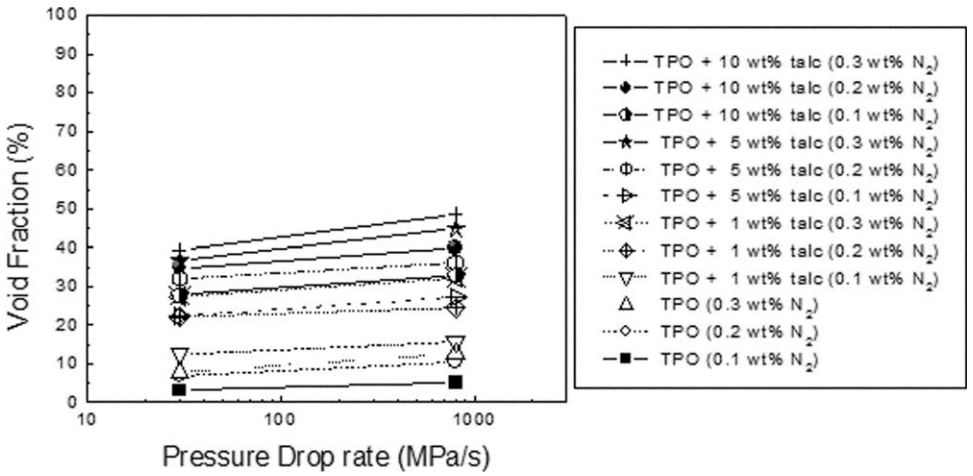


**Figure 17** Effect of the pressure-drop rate on the void fraction of the TPO foams.

concentration of $N_2$. Furthermore, the onset point of nucleation occurred earlier as the talc content increased.

Therefore, we concluded that, for low concentrations of $N_2$ and talc, the cell density was strongly affected by both $N_2$ and talc. When only the $N_2$ content or talc content was high, cell nucleation was governed by the parameter with the high content, regardless of the content of the other parameter. Therefore, as observed by Park et al.[25] the talc effect could not be observed in the case of a large amount of gas dissolved in the polymer matrix.

The cell density tended to level off above 10 wt % talc particles; this confirmed the observation made by Park et al.[25] This limiting effect might have been due to the agglomeration of talc particles. SEM micrographs of unfoamed talc-filled PP indicated that talc particles agglomerated to form large particles in the polymer matrix.[26] Therefore, it is possible that an increase in the talc concentration above 10 wt % did not actually create more effective nucleation sites.

## Foam extrusion

### Effects of the temperature on the cell density and void fraction

Figure 8(a,b) shows the cell density plotted against the die temperature. Regardless of the die geometry, the die temperature did not affect the cell density significantly in most cases; this supported the results reported by Xu et al.[2] In their study, the die temperature did not affect the cell nucleation density when all of the injected gas was completely dissolved in the polymer. In our experiment, we ensured the complete dissolution of $N_2$ in the polymer matrix by keeping the pressure much higher than the solubility pressure, as shown in Figure 9.[2,15] The cell density might have undergone deterioration as a result of gas loss because of the high melt temperature and cell coalescence and the low melt strength of TPO at high temperatures.[16,23,27] However, because a very small amount of $N_2$ was used in this study, the deterioration of cell density through bubble interactions (i.e., cell ripening, collapse, or coalescence) was negligible.

On the other hand, a fluctuation in the cell density was observed when the cell density was very low (i.e., $<10^3$ cells/cm$^3$). This variation was caused by the nonuniform distribution of bubbles, which is typically observed at a very low cell density.

The void fraction showed no sensitivity to the temperature.[21,24] Unlike the case of low-density foaming,[16,23] where the expansion ratio (or void fraction) is strongly dependent on gas loss at elevated temperatures, the void fraction was constant, regardless of the die temperature [see Fig. 10(a,b)]. This was due to the fact that the bubbles did not grow considerably (i.e., the cell-to-cell distance was large) because of the small amount of $N_2$ used in the high-density foaming process. Therefore, gas loss through cell-to-cell diffusion was not active, despite the high diffusivity at elevated temperatures.[21,24] This was a significant distinction because most foam manufacturers in industry attribute a low achieved void fraction to gas loss through the diffusion of a blowing agent to the atmosphere. Figure 10(a,b), however, clearly shows that this was not the case; this is a unique characteristic of high-density foaming.

### Effects of the talc content on the cell density and void fraction

Figure 11 outlines the effects of the talc content on the cell density. (Mean values were used for the cell density and the void fraction shown in Figs. 11–17.) The results obtained from both filamentary dies revealed a consistent trend: at low $dP/dt$ (pressure drop rate), the cell density increased gradually with

the talc content when 0.1 wt % $N_2$ was used; however, when 0.2 and 0.3 wt % $N_2$ were used, the cell density increased dramatically, even with 1 wt % talc. At high $dP/dt$, a significant increase in the cell density was observed even with 1 wt % talc. This tendency was due to the well-known heterogeneous nucleation effect, in which talc acts as a nucleating agent by decreasing the activation energy for cell nucleation.[28,29]

Figure 12 shows the void fraction as a function of the talc content. As in the case where the impact of 0.1 wt % $N_2$ on the cell density was considered, the void fraction here increased linearly with the talc content. Moreover, a sudden increase in weight reduction was again observed even when 1 wt % talc was used. We, thereby, surmised that the production of fine-celled TPO foams does not require a large amount of talc.

### Effects of the $N_2$ content on the cell density and void fraction

Figure 13 displays the cell density as a function of the $N_2$ content. The results obtained from both filamentary dies demonstrate a similar trend to those discussed previously. At 0.1 wt % $N_2$, a high cell density, over $10^5$ cells/cm$^3$, was obtained when 10 wt % talc was used. The results obtained from samples produced at two different pressure-drop rates showed a discrepancy in the case of low $N_2$ levels (0.1 wt %). At a low pressure-drop rate, the cell density was affected only by the talc content, regardless of the $N_2$ level; however, at a high pressure-drop rate, the cell density was additionally affected by the $N_2$ content. When a large amount (0.3 wt %) of $N_2$ was used, even a 1 wt % amplification in the quantity of talc increased the cell density dramatically. On the other hand, in the case of pure TPO, the cell density remained very low throughout the course of the experiments with both dies. When the $N_2$ content was increased to 0.3 wt %, the cell density did not increase significantly.

With respect to the void fraction, as shown in Figure 14, a slightly different result was observed. Regardless of the talc content, the void fraction increased linearly with the $N_2$ content. On the basis of the results pertaining to the cell density and void fraction, we expect that, for high-density foaming, a high $N_2$ content (0.2 wt %) will not be required as long as sufficient talc (5 wt %) is used.

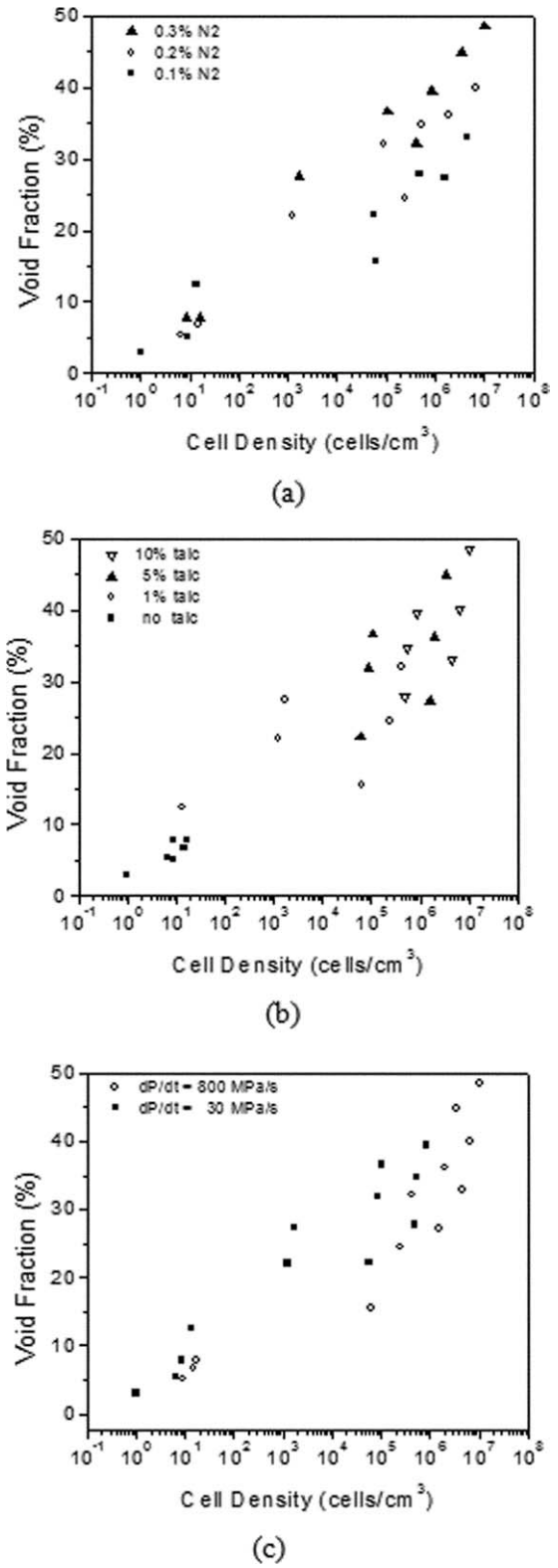


**Figure 18** Void fraction plotted against the corresponding cell density: effects of the (a) $N_2$ content, (b) talc content, and (c) $dP/dt$.

### Effects of the pressure-drop rate on the cell density and void fraction

It is commonly known that, in foam processing with $CO_2$, the cell density depends strongly on the pressure-drop rate;[2,14,15] for example, a higher pressure-drop rate increases the cell density.[2,14,15] To observe the effects of the pressure-drop rate on the cell density of foams blown with $N_2$, the cell densities were

plotted against the pressure-drop rates (Fig. 15). As mentioned previously, cell densities lower than $10^3$ cells/cm$^3$ were not reliable sources of data and were, thus, neglected.

The cell structures of the TPO foams with both $N_2$ levels and talc content are shown in Figure 16. Unlike the case of foams blown with $CO_2$, the cell density of the foams blown with $N_2$ increased only slightly as the pressure-drop rate increased (Figs. 15 and 16). It seemed that, for heterogeneous nucleation with $N_2$, the pressure-drop rate played a less significant role in cell nucleation compared to foaming with $CO_2$. Instead, talc was the dominant factor in determining the cell density. It was very interesting that talc still acted as a nucleating agent even at a very high pressure-drop rate ($\sim$ 800 MPa/s); this was not the case with $CO_2$.[2]

Furthermore, as the talc content increased, the sensitivity of the cell density to the pressure-drop rate decreased further. This last observation supported the fact that the pressure-drop rate did not play a significant role in heterogeneous cell nucleation, as discussed previously.

Similarly, the pressure-drop rate had no effect on the weight reduction, as shown in Figure 17. Weight reduction was determined only by the talc and $N_2$ contents.

### Relationship between the cell density and void fraction

The void fraction of the high-density foams increased with the cell density. That is, as the cells became more refined due to the large number of nuclei, the void fraction of the foam increased. To track the relationship between the cell density and void fraction, we plotted the void fraction against the corresponding cell density (Fig. 18). This figure reveals that the void fraction was a function of the cell density; this indicates that a high void fraction was achieved in high-density foaming when a high cell density was obtained, another characteristic unique to high-density foams.[21,24]

## CONCLUSIONS

In this study, batch foaming simulation experiments were performed with $N_2$ as a blowing agent. A batch foaming simulation system with a visualization component was used to effectively evaluate the foamability of TPO–talc composites. Using the visual observation apparatus, we observed the effects of talc on bubble nucleation. We quantitatively analyzed the bubble nucleation behaviors, revealing that cell density in the TPO composite increased with increasing talc content. At a low $N_2$ concentration, the effect of talc on the cell density was significant; at a high $N_2$ concentration, the cell density became insensitive to the talc concentration.

Foaming experiments were also performed in extrusion with $N_2$. Regardless of the pressure-drop rate, a cell density of $10^6$ cells/cm$^3$ was achieved with a large amount of talc. In addition, the experimental results demonstrate that the void fraction was a function of the cell density, not a function of the die temperature, unlike low-density foams.

The authors thank the Dow Chemical Co. for the kind donation of Engage materials.

## References

1. Park, C. B.; Liu, Y.; Naguib, H. E. Cell Polym 1999, 18, 367.
2. Xu, X.; Park, C. B.; Xu, D.; Pop-Iliev, R. Polym Eng Sci 2003, 43, 1378.
3. Lee, J. W. S.; Wang, K. H.; Park, C. B. Ind Eng Chem Res 2005, 44, 92.
4. Multicomponent Polymer Systems; Miles, I. S.; Rostami, S., Eds.; Longman Scientific and Technical: London, 1992.
5. Bucknall, C. B. Toughened Plastics; Applied Science: London, 1977.
6. Pramanick, A.; Sain, M. Polym Polym Compos 2006, 14, 455.
7. Sain, M.; Hudec, I.; Beniska, J.; Rosner, P. Mater Sci Eng A 1989, 108, 63.
8. Yu, T. C. Polym Eng Sci 2001, 41, 656.
9. Meiske, L. A.; Wu, S.; Sehanobish, K.; Dibbern, J. Soc Plast Eng Annu Tech Conf Tech Pap 1996, 2001.
10. Di Maio, E.; Mensitieri, G.; Iannace, S.; Nicolais, L.; Li, W.; Flumerfelt, R. W. Polym Eng Sci 2005, 45, 432.
11. Kim, S. G.; Kim, B. S.; Park, C. B. Cell Polym 2006, 25, 19.
12. Guo, Q.; Park, C. B. Soc Plast Eng Annu Tech Conf Tech Pap 2008, 2, 1008.
13. Klempner, D.; Frisch, K. C. Handbook of Polymeric Foams and Foam Technology; Hanser: New York, 1991.
14. Park, C. B.; Baldwin, D. F.; Suh, N. P. Polym Eng Sci 1995, 35, 432.
15. Park, C. B.; Suh, N. P. Polym Eng Sci 1996, 36, 34.
16. Naguib, H. E.; Park, C. B.; Reichelt, N. J Appl Polym Sci 2004, 92, 2661.
17. Han, J. H.; Han, C. D. Polym Sci Eng 1988, 28, 1616.
18. Taki, K.; Nakayama, T.; Yatsuzuka, T.; Ohshima, M. J Cell Plast 2003, 39, 155.
19. Taki, K.; Yanagimoto, T.; Funami, E.; Okamoto, M.; Ohshima, M. Polym Sci Eng 2004, 44, 1004.
20. Guo, Q.; Wang, J.; Park, C. B.; Ohshima, M. Ind Eng Chem Res 2006, 45, 6153.
21. Lee, J. W. S.; Park, C. B. Macromol Mater Eng 2006, 291, 1233.
22. Park, C. B.; Cheung, L. K. Polym Eng Sci 1997, 37, 1.
23. Li, G.; Gunkel, F.; Wang, J.; Park, C. B.; Altstadt, V. J Appl Polym Sci 2007, 103, 2945.
24. Lee, J. W. S.; Park, C. B.; Kim, S. G. J Cell Plast 2007, 43, 297.
25. Park, C. B.; Cheung, L. K.; Song, S. W. Cell Polym 1998, 17, 221.
26. Lee, S. T. Polym Eng Sci 1993, 33, 418.
27. Behravesh, A. H.; Park, C. B.; Pan, M.; Venter, R. D. Polym Prepr (Am Chem Soc Div Polym Chem) 1996, 37, 767.
28. Colton, J. S.; Suh, N. P. Polym Eng Sci 1987, 27, 485.
29. Leung, S.; Park, C. B.; Li, H. Plast Rubber Compos Macromol Eng 2006, 35, 93.